Copper(II) complexes of sulfonated salan ligands: thermodynamic, spectroscopic features and applications for catalysis of the Henry reaction

Szilvia Bunda [1,2], Nóra V. May [3*], Dóra Bonczidai-Kelemen [2,4], Antal Udvardy [1], H.Y. Vincent Ching[5], Kevin Nys[5], Mohammad Samanipour[5], Sabine Van Doorslaer[5], Ferenc Joó [1,6*], Norbert Lihi [4,6*]

[1] Department of Physical Chemistry, University of Debrecen, Debrecen, Hungary

[2] Doctoral School of Chemistry, University of Debrecen, Debrecen, Hungary

[3] Centre for Structural Science, Research Centre for Natural Sciences, Budapest, Hungary

[4] Department of Inorganic and Analytical Chemistry, University of Debrecen, Hungary

[5] Department of Chemistry, University of Antwerp, Universiteitsplein 1, Antwerpen, B-2610, Belgium

[6] MTA-DE Redox and Homogeneous Reaction Mechanisms Research Group, University of Debrecen, Debrecen, Hungary

* Correspondence: may.nora@ttk.mta.hu (N. V.M); joo.ferenc@science.unideb.hu (F. J.); lihi.norbert@science.unideb.hu (N. L.)

Abstract

Copper(II) complexes formed with sulfonated salan ligands (HSS) have been synthesized and their coordination chemistry has been characterized using pH-potentiometry and spectroscopic methods (UV-Vis, EPR, EDNMR) in aqueous solution. Several bridging moieties between the two salicylamine functions were introduced e.g., ethyl (**HSS**), propyl (**PrHSS**), butyl (**BuHSS**), cyclohexyl (*cis*-**CyHSS**, *trans*-**CyHSS**) and diphenyl (**dPhHSS**). All the investigated ligands feature excellent copper(II) binding ability *via* the formation of (O^{-},N,N,O^{-}) chelate system. The results indicated that the cyclohexyl moiety significantly enhances the stability of the copper(II) complexes. EPR studies revealed that the arrangement of the coordinated donor atoms is more symmetrical around the copper(II) center and similar for **HSS**, **BuHSS, CyHSS** and **dPhHSS**, respectively, and higher rhombicity of the ***g*** tensor was detected for **PrHSS**. The copper(II) complexes of the sulfosalan ligands were isolated in solid form, too, and showed moderate catalytic activity in the Henry (nitroaldol) reaction of aldehydes and nitromethane. The best yield for nitroaldol production was obtained for copper(II) complexes of **PrHSS** and **BuHSS**, although their metal binding ability is moderate compared to the cyclohexyl counterparts. However, these complexes possess larger spin density on the nitrogen nuclei than for the other cases, that alter their catalytic activity.

INTRODUCTION

Salen (1,2-bis(salicylaldiminato)ethane) is probably one of the most widely studied ligands in coordination chemistry. Since it contains a potential O,N,N,O donor atom set for tetradentate coordination, this ligand has been used mainly for complexation of hard metal ions such as Ni(II), Co(II/III) and Fe(II/III), although complexes with many other metal ions are also known. Metal-salen complexes also play a significant role in homogeneous catalysis.[1] With the recent upsurge of aqueous organometallic catalysis, there is a growing need to apply metal-salen complexes in aqueous systems, however, this is often hindered by the insolubility of such complexes in water. A possible solution to this problem is the attachment of ionic or highly polar substituents (such as sulfonate, carboxylate, ammonium, phosphonium, or oligoether groups) to the salen ligands.[2,3] Even then, the hydrolytic instability of the imine-type ligands still remains a major obstacle in their use in aqueous media. It has been unequivocally demonstrated, that extended use in aqueous reaction mixtures leads to the hydrolytic decomposition of metal-salen complexes.[2,4] Elimination of the C=N moiety in salen-derivatives by catalytic hydrogenation yields secondary amines which are stable to hydrolysis but still remain good complexing agents. These ligands, called *salans* (Scheme 1), have already served as catalysts for homogeneous transformations, and their use in aqueous reaction systems can be facilitated by appending to them ionic or polar substituents. An example is the use of hydrogenated sulfonated salens (i.e. *sulfosalans*, or *HSS*-type ligands) which are highly soluble in water while showing pronounced stability against hydrolytic decomposition.

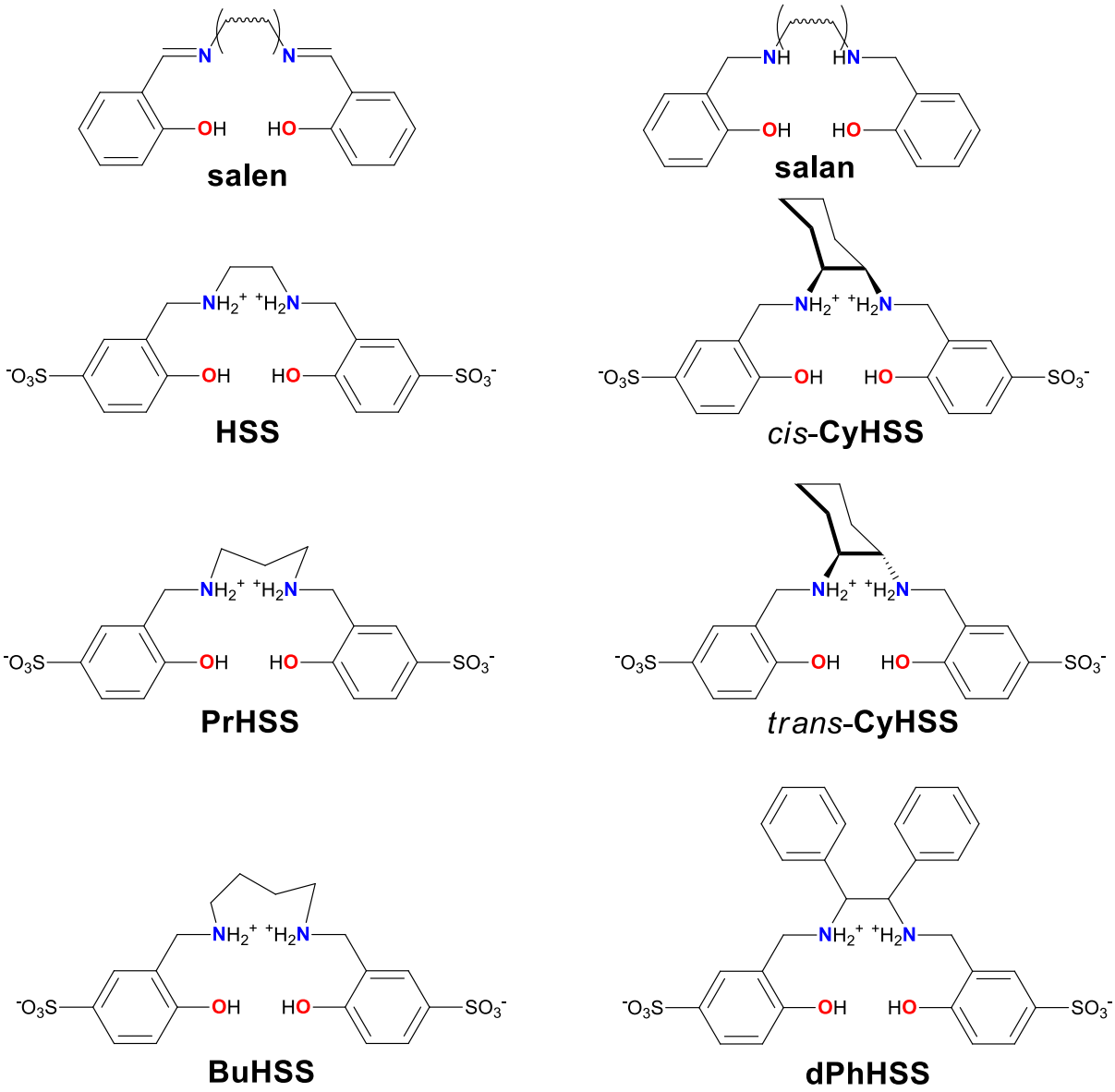

Scheme 1. General formulae of salen and salan type ligands and the structure of the sulfonated salans used in this study (H_4L).

Several studies have been published in the literature on the complex formation, biological and catalytic activities of certain salan complexes with metal ions such as Ti [5],V [2],Cr [6], Fe[7], and the state-of-the-art was expertly reviewed in 2019.[8] Variation of the linker group between the secondary nitrogen atoms in the salan molecules may give a possibility to fine-tune the electronic properties of the complexed metal ion and also the steric characteristics of the metal complex with obvious consequences on physical (e.g. spectroscopic) and chemical (e.g.

catalytic) behaviour of the molecule. With that aim in mind, a few studies of salan complexes included also the variation of the bridging unit.[9,10,11] Among the metal ions not previously reviewed, [8] Cu(II) is particularly useful for investigation of the formation, electronic and steric properties of its salan complexes, since – in addition to the usual spectroscopic methods (UV-vis, NMR, MS) – such complexes can also be probed by electron paramagnetic resonance (EPR) spectroscopy and its related hyperfine techniques, a sensitive tool to study paramagnetic systems.

In our laboratories, we have prepared a series of sulfosalans with various bridging units between the secondary nitrogen atoms.[9,10,12,13] Complex formation equilibria of some of these ligands were studied with Pd(II) [9,14] and Ni(II) [9] , however, most of our investigations were directed towards the catalytic properties of Pd(II)-salan complexes in C–C cross-coupling reactions in aqueous reaction mixtures.[10,12,13] It was assumed that knowledge of the distribution of the various complex species as a function of the pH could help in finding the optimal reaction conditions and might be instructive for the use of similar complexes of earth-abundant (instead of precious) metals in homogeneous catalysis. Indeed, we succeeded in developing the first process of hydrogenation and redox isomerization of allylic alcohols catalyzed by a Ni(II)-complex with an HSS-type ligand.[9] In another study, Pd(II)-complexes formed with an extensive series of sulfosalan ligands with various bridging units were applied for the Suzuki-Miyaura cross-coupling reaction of aryl halides with aryl boronic acid derivatives.[10,12]

Encouraged by the mentioned results of parallel coordination chemistry studies and catalytic investigations, we decided a closer investigation of the effect of the various linkers in the water-soluble sulfosalans on complex formation. A detailed EPR study has already been reported for chiral copper(II)-salen complexes[15], however, copper(II)-sulfosalan complexes have not been investigated before by use of simultaneous equilibrium and EPR techniques. Below, we report the equilibrium and structural study of Cu(II)-complexes with several HSS-type ligands, shown

in Scheme 1. Furthermore, the catalytic activity of these complexes was also studied in aqueous media in the Henry or nitroaldol reaction of aldehydes and nitroalkanes, a synthetically important C-C bond forming process.[16 17 18 19 20]

EXPERIMENTAL SECTION

Materials and methods. The $CuCl_2$ stock solution was prepared from the highest available grade and its concentration was checked gravimetrically and ICP method. The concentration of the sulfosalan ligands were checked by pH-potentiometry. For solution equilibrium and spectroscopic studies, doubly deionized and ultrafiltered (ELGA Purelab Classic system) water was used.

Synthesis of HSS-type ligands. The synthesis of the ligands was performed according to the methods established in the literature. **HSS** and **BuHSS** were prepared as described in Ref.[14] and *cis*-**CyHSS**, *trans*-**CyHSS** and **dPhHSS** were obtained as described earlier.[10] The synthesis of **PrHSS** was carried out analogously to the preparation of **HSS**; details were reported in our previous paper. [9] All ligands were identified on the basis of their ^{1}H and ^{13}C NMR spectra and they were excellent agreement with those reported earlier.[10] The purity of the ligands was also checked by pH-potentiometric titrations.

Synthesis and isolation of the Cu(II)-sulfosalan complexes. *General procedure.* 43.6 mg (0.24 mmol) of Cu(II)-acetate, $Cu(OAc)_2$ and 0.24 mmol of the appropriate sulfosalan ligand (L) were dissolved in water (4 mL). The pH was adjusted to 7.0 – 8.5 with concentrated NaOH, and the reaction mixture was stirred at 60 °C for 14 h. Then the solution was cooled to room temperature in ice water and the $Na_2[Cu(L)]$ product was precipitated by addition of 30 mL ice-cold ethanol. The solid was filtered, washed with absolute ethanol, and dried under vacuum. The products were characterized by UV-visible and FTIR spectroscopies and by HR ESI-MS method. For details of the synthesis of Na_2[Cu(**HSS**)] (**1**), Na_2[Cu(**PrHSS**)] (**2**), Na_2[Cu(**BuHSS**)] (**3**) Na_2[Cu(*cis*-**CyHSS**)] (**4**), Na_2[Cu(*trans*-**CyHSS**)] (**5**), and Na_2[Cu(**dPhHSS**)] (**6**) and for the respective spectroscopic data see Supporting Information.

pH-potentiometry. The protonation constants (pK_a) of the sulfosalan ligands and the overall stability constants (logβ_{pqr}) of the copper(II) complexes were determined by pH-potentiometric titration method using a carbonate free KOH solution (ca. 0.5 M). The carbonate contamination was determined using the appropriate Gran functions.[21] 10 mL aliquots of the ligands (ca. 4 mM) were titrated, the ionic strength of the samples was adjusted to 0.2 M KCl and the equilibrium measurements were carried out at 298 K. The samples were stirred using a magnetic stirrer. During the titrations, the headspace and the sample were purged with argon in order to ensure the absence of oxygen and carbon-dioxide. The pH measurements were made using a computer-controlled *Metrohm 785 DMP Titrino* automatic titrator and the instrument was equipped with a *Metrohm 6.0262.100* combination glass electrode. The pH reading was converted to hydrogen ion concentration as described by Irving et al.[22] The protonation constants (pK_a) of the ligands and the overall stability constants of the metal complexes, $\beta_{pqr} = [Cu_pL_qH_r]/[Cu]^p[L]^q[H]^r$, were calculated by using the dedicated computational programs, SUPERQUAD [23] and PSEQUAD.[24] The distribution curves of the complexes formed between copper(II) and the ligands were calculated by the use of computational program, MEDUSA.[25]

UV-Vis, CD and FTIR spectroscopic methods. UV-visible spectra of the copper(II) complexes were recorded with an Agilent Technologies Cary 60 UV-VIS xenon pulse lamp spectrophotometer in the 250 – 800 nm wavelength range using the same concentration range as in the pH-potentiometric titrations. The circular dichroism spectra were registered with a Jasco J-810 spectropolarimeter using 1 mm and/or 1 cm cells in the 250 – 800 nm wavelength range. Individual samples were prepared for UV-vis and CD experiments. Infrared spectra were recorded on a Perkin Elmer Spectrum Two FT-IR Spectrometer in ATR mode.

CW-EPR measurements and simulation of the spectra. All CW-EPR spectra were recorded with a BRUKER EleXsys E500 spectrometer (microwave frequency 9.45 GHz, microwave power 13 mW, modulation amplitude 5 G, modulation frequency 100 kHz). Anisotropic EPR

spectra were recorded for aqueous solutions containing 5 mM copper(II)chloride and 5 mM sulfosalan ligands. NaOH solution was added to the stock solution to adjust the pH of the samples. An 0.1 mL aliquot of sample solution was introduced into a quartz EPR tubes then 0.025 mL MeOH was added to avoid water crystallization upon freezing. Frozen solution EPR spectra were measured in a Dewar container filled with liquid nitrogen at 77 K. The measured spectra were corrected by the baseline spectrum measured in the same way and simulated using a designated EPR program. [26] To describe the isotropic spectra the parameters g_0, A_0^{Cu} copper hyperfine (^{63,65}Cu, I= 3/2) couplings were fitted and two equivalent a_0^N nitrogen (^{14}N, I = 1) superhyperfine couplings have been taken into account with the parameters determined by EDNMR measurements. The relaxation parameters, α, β, and γ defined the linewidths through the equation $\sigma_{MI}=\alpha+\beta M_I+\gamma M_I^2$, where M_I denotes the magnetic quantum number of the paramagnetic metal ions. For *trans*-**CyHSS** and **dPhHSS** spectra, the four lines were fitted with separate linewidth values (ω_1- ω_4).

The anisotropic EPR spectra, recorded at 77 K, were also analyzed with the EPR program. Rhombic ***g***-tensor (g_x, g_y, g_z) and rhombic copper hyperfine tensor (A_x^{Cu}, A_y^{Cu}, A_z^{Cu}) were fitted to simulate the spectra. Rhombic nitrogen hyperfine tensor (a_x^N,a_y^N,a_z^N) obtained by EDNMR was used in the simulation without fitting these parameters. For the description of the linewidth, the orientation dependent α, β and γ parameters were used to set up each component spectra. In order to check the correctness of the evaluation, the solution spectra have been described also by using the anisotropic EPR values and fitting the rotational correlation times. Since a natural copper(II)chloride was used for the measurements, both the isotropic and anisotropic spectra were calculated as the sum of the spectra of ^{63}Cu and ^{65}Cu weighted by their natural abundances. The hyperfine and superhyperfine coupling constants and the relaxation parameters were obtained in field units (Gauss = 10^{-4} T).

Pulsed-EPR measurements. ESE-detected EPR and ELDOR (Electron electron double resonance)-detected NMR (EDNMR) measurements [27] [28] were carried out with a W-band (95 GHz) Bruker ELEXSYS E680 spectrometer in conjunction with a split-coil Oxford 6T superconducting magnet equipped with an Oxford flow cryostat and a Bruker cylindrical cavity at 6 K. For the EDNMR measurements, the pulse sequence was $HTA_{mw2} - T - \pi/2_{mw1} - \tau - \pi_{mw1} - \tau -$ echo sequence, with the length of the high-turning angle (HTA) pulse 20 μs, $t_{\pi/2}$ = 200 ns, and t_{π} = 400 ns. Delay times of T = 4.4 μs and τ = 848 ns were applied. Spectra were recorded at 5−6 different observer positions, with 20−45 scans for each spectrum depending on the echo intensity. The samples were prepared in water using 0.83 mM complex concentration and glycerol was used to avoid water crystallization. NaOH was added to the samples by adjusting the pH (around pH 8.0).

The EDNMR and ESE-detected EPR spectra were simulated using the EasySpin open-source MATLAB toolbox (version 5.2.28). [29]

Mass spectrometry and NMR spectroscopy. ESI-TOF-MS measurements were made with a Bruker maXis II MicroTOF-Q type Qq-TOF-MS instrument (Bruker Daltonik, Bremen, Germany) both in negative and positive modes. The instrument was equipped with an electrospray ion source where the spray voltage was 4 kV. N_2 was utilized as a drying gas and the drying temperature was 200 °C. The spectra were accumulated and recorded using a digitalizer at a sampling rate of 2 GHz. The mass spectra were calibrated externally using the exact masses of sodium formate clusters. The spectra were evaluated using DataAnalysis 4.4 software from Bruker.

360 MHz ^{1}H NMR spectra were recorded on a Bruker Avance DRX spectrometer at 298 K. The chemical shifts were referenced to sodium trimethylsilylpropanesulfonate (DSS) dissolved in the sample and D_2O was used as a solvent.

Single crystal X-Ray diffraction (SC-XRD) measurements. Diffraction measurements of K_2[Cu(**PrHSS**)]×3H_2O were made on a Bruker D8 VENTURE Dual source X-ray Diffractometer with Mo Kα (λ = 0.71073 Å) radiation. The structure was solved and refined with the use of SHELX program sets [30,31] managed by the OLEX^2. [32] Data were analysed by PLATON [33], graphics were prepared with the Mercury [34] and OLEX^2 software.

The crystallographic data (including structure factors) were deposited in the Cambridge Crystallographic Data Centre (CCDC) with No 2071125.

Catalytic Henry reactions - Typical procedure.

In a Schlenk tube, 0.025 mmol Cu(II)-sulfosalan catalyst was dissolved in 2 mL solvent (water or a 1/1 (v/v) water/methanol mixture) followed by addition of 135 μL (2.5 mmol) nitromethane and 51 μL (0.5 mmol) benzaldehyde. The reaction mixtures were magnetically stirred at 75 °C in air. After the desired reaction time, the mixture was cooled in ice water and extracted with 2 mL dichloromethane. The phases were separated, the organic phase was dried by passing through a short Na_2SO_4 plug and evaporated to dryness on a rotary evaporator. The residue was taken up in $CDCl_3$ and subjected to ^{1}H NMR measurement. Conversions were determined by the integration of the formyl proton (*H*(C=O)) and alcoholic OH (C-O*H*) proton signals in benzaldehyde and in the nitroaldol product, respectively.

For catalysis of the Henry reaction with *in situ* prepared complexes, 0.24 mmol of the appropriate sulfosalan and 43.60 mg (0.24 mmol) of $Cu(OAc)_2$ were dissolved in water (4 mL). The pH was adjusted to 7.0 – 8.5 with 1 M NaOH, and the solution was stirred at 60 °C for 2 h. Aliquots of such stock solutions were used to catalyse the Henry coupling reaction. ESI-MS spectra of these stock solutions were identical to those prepared by dissolution of isolated complexes.

RESULTS AND DISCUSSION

Equilibrium and structural studies in solution

Acid-base equilibria

Deprotonation constants of **HSS**, **PrHSS** and **BuHSS** have already been published earlier and the different sets of data show excellent agreement. [2,9] Moreover, the thorough analysis of the deprotonation microprocesses was also published for these ligands.[9] The acid dissociation constants of the ligands were determined by fitting the pH-potentiometric data and are collected in Table 1.

Table 1. Stepwise deprotonation constants (pK_a) of the ligands [a]
(I = 0.2 M KCl, T = 298 K)

	HSS [b]	**PrHSS** [b]	**BuHSS** [b]	*cis*-**CyHSS**	*trans*-**CyHSS**	**dPhHSS**
H_4L	6.00	6.93	6.94	4.32(5)	4.45(4)	6.13(6)
H_3L	7.44	7.82	7.81	7.71(4)	7.65(4)	6.68(7)
H_2L	8.75	9.57	10.08	9.10(4)	9.13(4)	9.33(6)
HL	10.64	11.28	11.47	11.42(2)	11.37(2)	9.86(6)
ΣH_iL	32.83	35.60	36.30	32.55	32.60	32.00

[a] 3σ standard deviations are in parentheses. [b] Data are taken from Ref. [9]

In accordance with the structure of the ligands, the sulfonic acid groups, the two phenolic–OH groups and the secondary ammonium functions are involved in acid-base processes. From these groups, the deprotonation of sulfonic acid groups occurs below pH < 1.5, thus it falls out from the potentiometrically measurable pH-range. Consequently, H_4L denotes the ligands where the two phenolic–OH groups and the secondary ammonium functions are protonated.

It was found that the acidity of the secondary ammonium group significantly enhances for the cyclohexyl-bridged ligands, (*cis*-**CyHSS** and *trans*-**CyHSS**). This is most probably due to the electron-donating effect of the cyclohexyl moiety. The formation of intramolecular hydrogen bond between the secondary amine group and protonated phenolic hydroxyl group is more pronounced in these systems than for **HSS**, **PrHSS**, **BuHSS** and **dPhHSS**, respectively (see Table 1., H_4L). Consequently, the first deprotonation step is separated from the subsequent deprotonation processes. Such behavior has already been published for sulfosalan ligands containing tertiary amine moiety.[35] Upon increasing the pH, the further deprotonation steps significantly overlap. On the basis of earlier literature data, it is reasonable to assume that the subsequent process is mainly associated to the deprotonation of the second hydroxyl group,

while the highest pK_a value is assigned to the deprotonation of secondary ammonium group. These deprotonation microprocesses are illustrated in Scheme S1.

In addition, the acid-base properties of the two cyclohexane isomers are the same, therefore the relative positions of the amine groups do not have significant effect on this feature. Moreover, X-Ray diffraction studies were reported on these ligands. It was shown that the two cyclohexyl rings precisely overlap and only the position of the aromatic rings is different in solid phase. [10]

Copper(II) complexes

Equilibrium studies. The complex formation processes between copper(II) and the ligands were studied by the pH-potentiometric method and the stability constants of the corresponding complexes are reported in Table 2. The representative concentration distribution curves of the species formed in the Cu(II)/**HSS** and Cu(II)/*trans*-**CyHSS** are shown in Figure 1 while similar distributions for the systems examined are reported in the Supporting Information (Figure S1-S4).

Table 2. Stability constants of the complexes formed between copper(II) and the sulfosalan ligands. [a] (I = 0.2 M KCl, T = 298 K)

	HSS	**PrHSS**	**BuHSS**	***cis*-CyHSS**	***trans*-CyHSS**	**dPhHSS**
$[CuLH]^{-}$	24.25(1)	24.82(1)	22.04(1)	26.25(1)	26.70(1)	
$[CuL]^{2-}$	20.34(1)	18.98(1)	15.70(1)	21.96(5)	22.65(2)	17.75(6)
pCu	8.43	5.74	3.67	8.76	9.51	6.42
pK_{CuL}^{CuLH}	3.91	5.84	6.34	4.29	4.05	

[a] 3σ standard deviations are in parentheses.

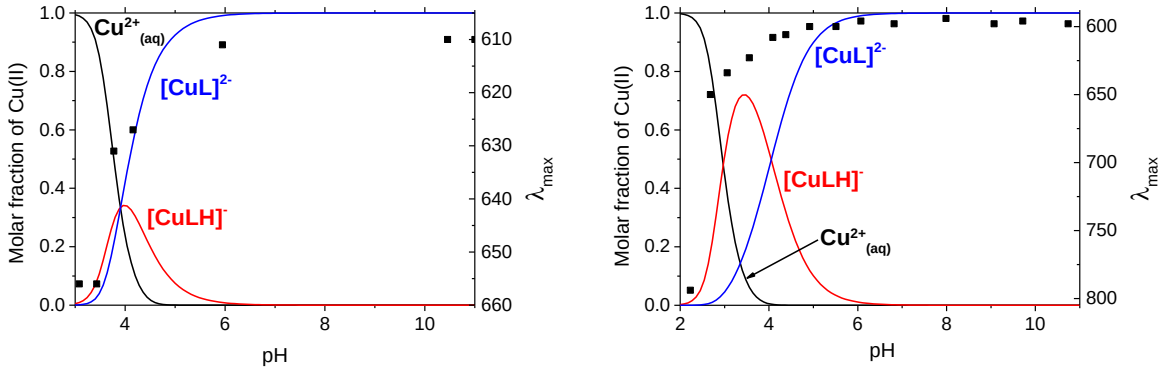

Figure 1. Distribution of the complexes formed in the Cu(II)/**HSS** (left) and Cu(II)/*trans*-**CyHSS** (right) 1/1 systems and the λ_{max} values at the *d-d* band (■) obtained by UV-vis spectroscopy as a function of pH (I = 0.2 M KCl, T = 298 K). c_L = 2 mM

The equilibrium model used for the fitting of the pH-potentiometric data was confirmed by pH-dependent UV-vis titration. A comparison of the λ_{max} values of the *d–d* transition (*vide infra*) with the species distribution curves calculated on the basis of the stability obtained by pH-potentiometric titrations confirms that the equilibrium model applied for the refinement of the

data set is correct. The equilibrium is described by considering the formation of $[CuL]^{2-}$ and monoprotonated $[CuLH]^{-}$ species for all systems except that of **dPhHSS**.

In the slightly acidic pH-range, the complex formation reactions start with the $[CuLH]^{-}$ complexes. In these complexes, the coordination sphere of the copper(II) is accommodated by the (O^{-},N,N) donor set. The metal center possesses a (6,5) membered chelate system with **HSS**, *cis*-**CyHSS**, *trans*-**CyHSS** and **dPhHSS,** while (6,6) and (6,7) membered chelate systems form with **PrHSS** and **BuHSS**, respectively. It is noteworthy to mention that although the secondary amine groups are the most basic sites in the ligands, the formation of (O^{-},N,O^{-}) mode is unlikely. Such coordination mode hinders the formation of linked chelate system which is not favorable with respect to thermodynamic point.

Upon increasing the pH, the next process provides the formation of (O^{-},N,N,O^{-}) coordinated complex ($[CuL]^{2-}$). The stepwise deprotonation constants for the formation of $[CuL]^{2-}$ (pK_{CuL}^{CuLH} in Table 2) are the highest for **PrHSS** and **BuHSS**. This feature can readily be explained by considering the fact that the increasing size of the bridging unit between the two salicylamine moieties in **PrHSS** and **BuHSS** shifts the deprotonation and coordination of the phenolic-OH group into the less acidic pH range. In addition, the stability constants of the corresponding copper(II) complexes exhibit decreasing tendency by increasing the bridging unit which is due to the size of the linked chelate system ((6,5,6) for **HSS** *vs.* (6,7,6) for **BuHSS**). Although **dPhHSS** forms a (6,5,6) linked chelate system with copper(II), its stability is significantly lower than that of **HSS**. This is most probably due to the presence of two aromatic moieties which results in repulsive forces between the neighboring aromatic systems.

The overall basicity of the investigated ligands differs (see Table 1), therefore the direct comparison of the stability constants does not provide essential information on the metal-binding ability of the sulfosalan ligands. In order to get reliable information on this feature, conditional stability constants and theoretical distribution curves were calculated. On the basis

of the calculated pCu values (pCu = –log $[Cu^{2+}]_{free}$ of the complexes at pH 7.4 using 10 μM Cu(II) and ligand concentrations), the investigated ligands exhibit a trend of copper(II) ion affinity which is as follows: *trans*-**CyHSS** > *cis*-**CyHSS** > **HSS** > **dPhHSS** > **PrHSS** > **BuHSS**. The distribution curves of the multicomponent system containing copper(II) and all of the investigated ligands in equimolar solution (Figure 2) unambiguously proves that the most effective copper chelators are the *trans*-**CyHSS** and *cis*-**CyHSS** ligands. **HSS** and **BuHSS** also contribute to the metal binding, however, this feature is negligible for **PrHSS** and **dPhHSS**. It is an interesting issue why the *trans*-**CyHSS** forms the most stable complexes and the copper(II) complexes of *cis*-**HSS** possess lower stability. Most probably, the *trans* positions of the amine groups are more favorable to accommodate the metal ion than that of *cis* position or the formation of conformation isomers can also be envisioned. In order to confirm this presumption, further spectroscopic measurements were carried out.

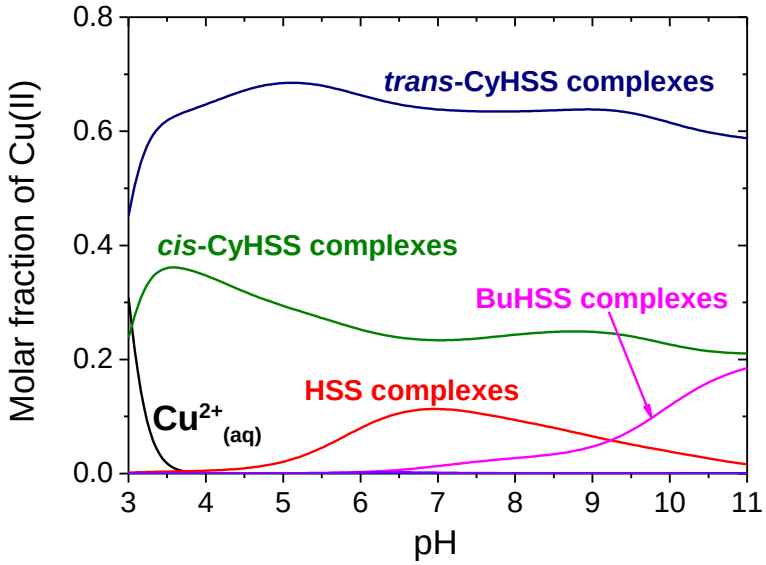

Figure 2. Theoretical distribution curves between copper(II) and all of the investigated ligands at equimolar solution as a function of pH. Copper(II) complexes of **PrHSS** and **dPhHSS** are not shown due to their negligible contribution to the metal binding. $c_{Cu(II)}$ = 2 mM

Mass spectrometry and electronic absorption spectroscopy. First, the MS spectra of the copper(II) complexes were registered at pH ~ 8, where the $[CuL]^{2-}$ complexes are the unique

species in all systems examined in this work. In all cases, the corresponding $[CuL]^{2-}$ complexes were observed, and the MS spectra do not exhibit any indication for the formation of dimeric or bis-ligand species and the major peaks are attributed to the mononuclear copper complexes and to the ligands (Figure S5-S10). The observed and calculated isotope patterns were in good agreement confirming the existence of the postulated species (Table S1). Noticeably, the negative ion mode used in these experiments leads to the formation of Cu(I)-sulfosalan complexes. Such outer sphere reduction mechanism has already been observed for several copper(II) complexes in gas phase under MS conditions, which happens in the electrospray source, when a high electric field is applied between the capillary and the counter electrode. [36] Since the non-spherical symmetry and the Jahn-Teller effect of the d^9 ground state of copper(II) can contribute to the stereochemistry of copper(II) complexes, the determination of the geometry is not a trivial task.[37] However, the thorough analysis of the electronic absorption spectra offers the possibility to study the geometry of the complexes formed in aqueous solution.[38]

The electronic absorption spectra of the copper(II)/sulfosalan ligands were registered as a function of pH. As a representative example, the pH-dependent UV-vis spectra of the copper(II)/*trans*-**CyHSS** system are reported in Figure 3.

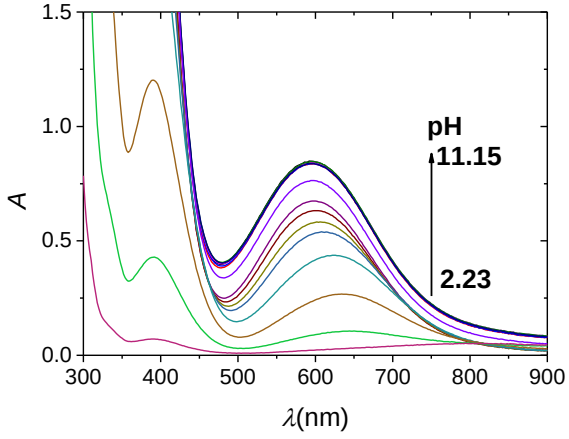

Figure 3. pH dependent UV-vis spectra for the Cu(II)/*trans*-**CyHSS** 1/1 system as a function of pH. c_L = 2 mM.

The UV-vis spectra of the investigated systems feature two significant absorptions that can be assigned as the *d* – *d* transition (around 600 nm, between 100 – 550 $M^{-1}cm^{-1}$) and the copper(II) – phenolate metal to ligand charge transfer band (around 390 nm, between 1000 – 2000 $M^{-1}cm^{-1}$).

The λ_{max} values with their corresponding molar absorptivity are reported in Table S2 and the set of data are in good agreement with those obtained for similar systems. It is clear from Table S2, that the λ_{max} values of the *d* – *d* transition are within the range of non-centrosymmetric square-planar copper complexes with a (O^-,N,N,O^-) donor set and are similar to those reported for similar complexes.[11,39] Although, the copper(II)ion is accommodated by the (O^-,N,N,O^-) donors in all cases, the λ_{max} values as well as the molar absorptivity values of the investigated complexes slightly differ. This is due to the distortion of the geometry around the metal center and symmetry considerations; if the distortion is small, the absorption becomes sharper and more intense, while its maximum shifts to higher energy values.[40] The same situation is expected for the copper(II) complex of *trans*-**CyHSS**, hence the distortion is small resulting in a decrease in the λ_{max} value. On the contrary, a rhombic distortion excludes higher absorption maxima for **PrHSS**.

It is important to note, that the ligands (*trans*-**CyHSS** and *cis*-**CyHSS)** and their copper(II) complexes contain stereocenters, thus their copper(II) complexes may exhibit optical activity. In an attempt, the circular dichroism spectra of these complexes were registered. Unfortunately, no optical activity was observed by use of CD spectroscopy (data not shown), indicating that the complexation with copper(II) yielded racemic mixtures.

X-band CW-EPR and W-band pulsed EPR studies. Solution X-band CW-EPR spectra recorded in equimolar metal and ligand concentration at room temperature, have been simulated by the designated EPR program. [26] The best spectral fit is shown in Figure 4 and the isotropic EPR parameters are collected in Table 3 (the linewidth parameters are reported in Table S3).

Table 3. EPR parameters obtained for the copper(II)-sulfosalan ligands in aqueous solution.

Complex	**Isotropic EPR parameters**[a]		**Anisotropic EPR parameters**[b]		**Isotropic EPR param.**[c]	
	g_0	A_0 /×10^{-4} cm^{-1}	g_x, g_y, g_z	A_x^{Cu} ,A_y^{Cu}, A_z^{Cu} / ×10^{-4} cm^{-1}	g_z/A_z / ×10^{-4} cm^{-1}	$g_{0,calc.}$[c]
[Cu(**HSS**)]$^{2-}$	2.109	80	2.041, 2.055, 2.240	35, 15, 186	122	2.112
[Cu(**PrHSS**)]$^{2-}$	2.114	72	2.044, 2.065, 2.246	25, 28, 176	128	2.118
[Cu(**BuHSS**)]$^{2-}$	2.110	78	2.040, 2.055, 2.240	36, 25, 185	121	2.108
[Cu(*cis*-**CyHSS**)]$^{2-}$	2.107	79	2.035, 2.053, 2.237	31, 25, 185	120	2.107
[Cu(*trans*-**CyHSS**)]$^{2-}$	2.089	68	2.037, 2.051, 2.233	30, 23, 186	120	2.107
[Cu(**dPhHSS**)]$^{2-}$	2.087	62	2.038, 2.050, 2.230	36, 15, 187	121	2.106
7 [d]			2.038, 2.057, 2.235	36.4, 10.6, 189.3	118	2.110
8 [d]			2.057, 2.033, 2.237	26.4, 18.5, 189.9	118	2.109
9 [d]			2.037, 2.055, 2.239	28.3, 22.5, 184.9	121	2.110
10 [d]			2.038, 2.056, 2.238	36.1, 7.8, 184.9	121	2.111

[a] The experimental error were ± 0.001 for g_0 and ± 1.0 cm^{-1} for A_0. [b] Recorded in 80 % H_2O/MeOH solvent mixture. The experimental error were ± 0.002 for g_x,g_y and ± 0.001 for g_z, ± 2×10^{-4} cm^{-1} for A_x and A_y and ±1×10^{-4} cm^{-1} for A_z. [c] Calculated by the equation $g_{0,calc} = (g_x+g_y+g_z)/3$ on the basis of anisotropic values. [d] Data are taken from Ref. [11] Structures of the copper(II) complexes are shown in the Supporting Information, Scheme S2. **7**: Cu^{II}[salan-(R,R-cyclohexane)]; **8**: Cu^{II}[methoxivanilin-(R,R-cyclohexane)]; **9**: Cu^{II}[methoxivanilin-(S,S-diphenylethane-1,2-diamine)]; **10**: Cu^{II}[3,5-di-tercbuthylsalan-(S,S-cyclohexane)].

The spectra were fitted with isotropic g_0 and A_0 parameters taking into account two equivalent nitrogen atoms (a_0^N) with parameters obtained by EDNMR results (*vide infra*). In general, the obtained spin-Hamiltonian parameters are in good agreement with those reported for similar

copper(II) complexes.[35,41,42] Moreover, the relationship between the *g*-tensors reported in Table 3 ($g_z > g_x, g_y > 2.0$) indicates the presence of $d_{x^2-y^2}$ ground state of copper in a square-planar or square-pyramidal coordination environment where most likely the axial position is accommodated by the solvent molecule.[43]

The spectra and the simulated EPR parameters show high similarity for the Cu(II) complexes of **HSS** and **BuHSS;** however, the data for the copper(II) complex of **PrHSS** differ significantly. The higher g_0 and lower A_0 values reflect lower ligand field around the copper(II) center in case of the **PrHSS** complex compared to those formed with **HSS** or **BuHSS**. These results are coherent with the λ_{max} values obtained by UV-vis spectroscopy and confirm the distortion of the geometry for copper(II) complex of **PrHSS**.

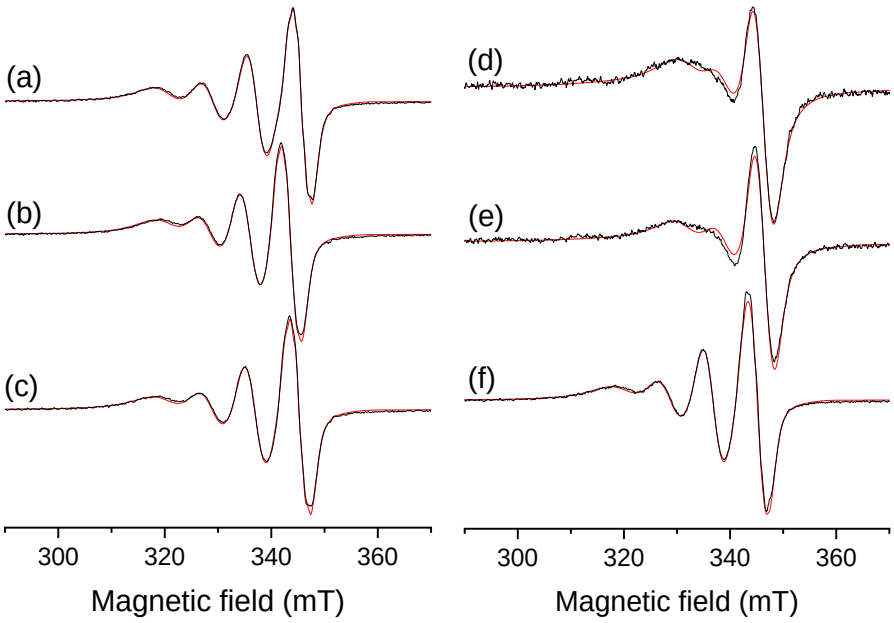

Figure 4. Experimental (black) and simulated (red) X-band CW-EPR spectra of the CuL complexes formed in the copper(II)-sulfosalan systems at 298 K in solution, for ligands (a) **HSS**, (b) **PrHSS**, (c) **BuHSS** (d) **dPhHSS** (e) *trans*-**CyHSS** (f) *cis*-**CyHSS**.

The line broadening detected in the solution spectra of the Cu(II) complex of **dPhHSS** is most probably due to the rotational inhibition induced by the large substituents. This was also confirmed by fitting the rotation correlation times on the basis of anisotropic EPR parameters, Figure S11. The rotation correlation time for Cu(II)/**dPhHSS** is approximately one order of

magnitude higher than those obtained for other complexes examined. Noticeably, the rotation correlation time for Cu(II)/*trans*-**CyHSS** is higher than that of *cis* counterpart. Based on the similar size of the ligands this is unlikely, instead, the possibility arises that the line broadening can originate from the coexisting of structural isomers for the *trans*-**CyHSS** complexes in solution at room temperature. In order to investigate the coordination geometry more in detail, anisotropic EPR spectra have been measured in frozen solution at pH = 7.0. The anisotropic spectra were simulated with rhombic ***g***- and copper hyperfine ***A***-tensor parameters (Table 3). Since the perpendicular part of the EPR spectra of the copper(II) complexes (3200 – 3350 G in Figure 5) does not allow the accurate determination of the rhombic nitrogen superhyperfine coupling values, these have been determined by W-band EDNMR experiments and were kept constants during the fitting and simulation of X-band EPR spectra (Table 4). In comparing the obtained values **PrHSS** also exhibited a lower copper hyperfine A_z value (176.1×10^{-4} cm^{-1}). Higher values were found for **HSS** and **BuHSS** (186.2 and 184.8×10^{-4} cm^{-1}, respectively). Beside the lower A_z value, the anisotropy of the ***g***-tensor is higher for the copper(II) complex of **PrHSS**, as g_x and g_y differ considerably (2.044 and 2.065), while they are less anisotropic for the Cu(II) complex of **HSS** (2.041 and 2.055) and **BuHSS** (2.040 and 2.055). According to these values, it is reasonable to assume that the arrangement of the coordinated donor atoms is more symmetrical and similar in **HSS** and **BuHSS** and higher rhombicity was detected for **PrHSS**.

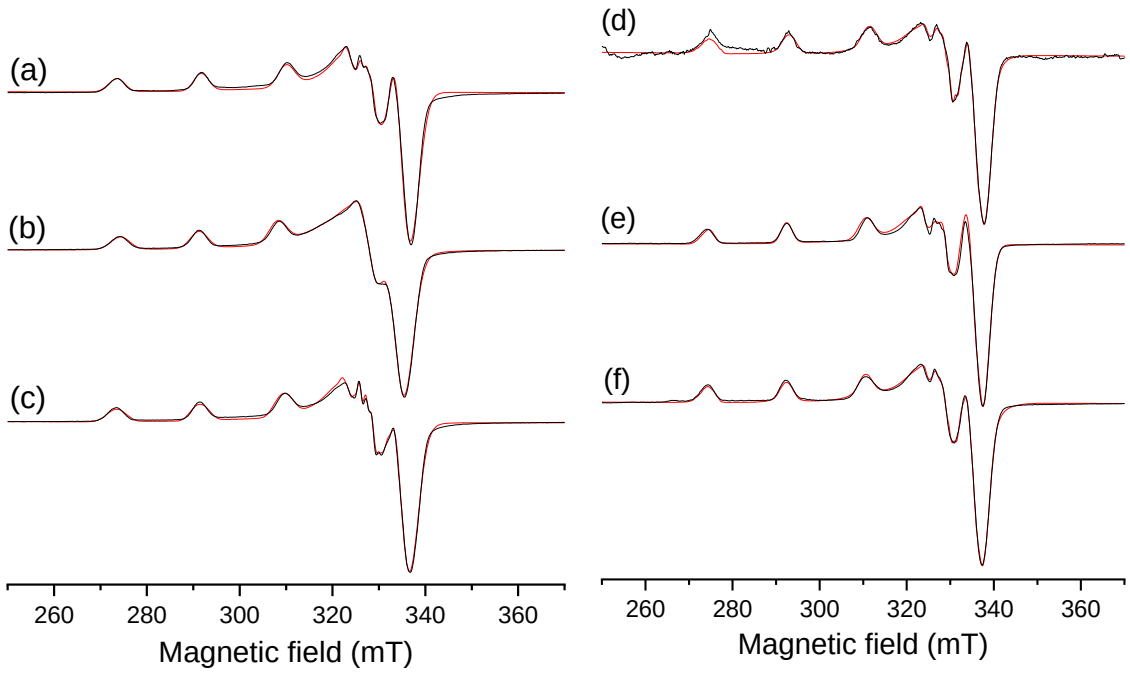

Figure 5. Frozen solution X-band CW-EPR spectra (black) of the CuL complexes formed in the copper(II)-sulfosalan systems at 77 K. (a) **HSS**, (b) **PrHSS** (c) **BuHSS** (d) **dPhHSS** in 67% DMSO/H_2O, (e) *trans*-**CyHSS** in 80% H_2O/MeOH and (f) *cis*-**CyHSS** in 80% H_2O/MeOH. Simulated EPR spectra (red) calculated from the spin-Hamiltonian parameters (reported in Table 3) obtained by the fitting of the spectra.

The introduction of electron donating substituents on the sulfosalan backbone results in slight changes in the EPR parameters. Somewhat lower g_0 and g_z values can be due to the effect of the electron donation in *cis*-**CyHSS**, *trans*-**CyHSS** and **dPhHSS.** According to the method established by Peisach-Blumberg[44,45] the g_z/A_z ratio gives a rough measure for the tetragonal distortion, although it must be noted that the g_z and A_z values are also influenced by the coordination number, the nature of the ligands and the dielectric constant of the solvent (Table 3). All g_z/A_z values of the complexes under study fall in the range between 120 – 130 in agreement with square-planar or square pyramidal (with axial coordination of solvent molecule) geometries of the copper(II) complexes. Comparison with the values reported for Cu(II) salen complexes in non-coordinating solvents with and without addition of an amine ligand,[15] the values indicate solvent ligation (*vide infra*). Figure 6(a) shows the plot of g_z as a function of

λ_{max} which are correlated and shows a decrease in the ligand field in the order: **dPhHSS** > *cis*-**CyHSS** > **BuHSS** ~ **HSS** > **PrHSS**. The *trans*-**CyHSS** gave an outlier value, according to λ_{max} it shows the highest ligand field though the g_z value was found similar to *cis*-**CyHSS**. As the λ_{max} was measured at room temperature and g_z in frozen solution we believe that the copper(II) complex of *trans*-**CyHSS** has structural isomers appearing in solution. This would also explain the much wider solution EPR spectrum of the *trans* form in comparing to the *cis* isomers.

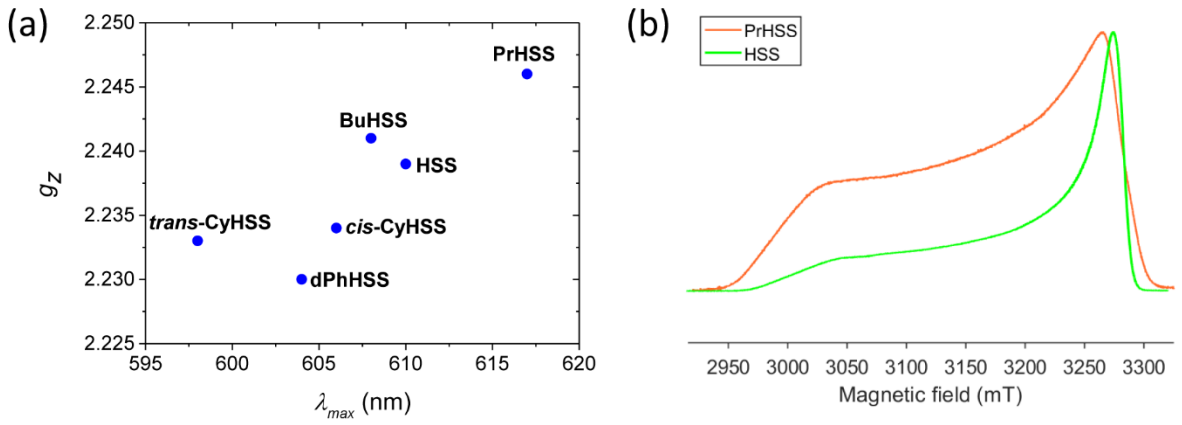

Figure 6. (a) Representation of g_z values of the CuL complexes as a function of λ_{max} values. (b) Comparison of the W-band ESE-detected EPR spectra recorded at 6 K for complexes [Cu(**HSS**)]$^{2-}$ and [Cu(**PrHSS**)]$^{2-}$. The spectra are shown normalized to highlight the strong difference in *g*-tensor anisotropy between the two complexes.

In order to compare the spin-Hamiltonian parameters of the complexes in more details, W-band ESE-detected EPR (Figure 6b, FigureS12) and EDNMR spectra have been recorded (Figure 7, S12-S16). EDNMR is a pulsed EPR technique based on the use of pulses with different microwave frequencies which allows to detect the nuclear transitions and thus unravel the hyperfine and nuclear quadrupole interactions of the magnetic nuclei interacting with the unpaired electron.[28] The position of the peaks detected in these spectra of the Cu(II) complexes reflects the ^{14}N and copper hyperfine and nuclear quadrupole couplings. Experiments were conducted at specific magnetic field positions shown together with the high-field ESE-detected EPR spectra in Figure S12. Figure 7 shows the part of the EDNMR spectra (after baseline correction) reflecting the ^{14}N nuclear transitions within the $M_S = -1/2$ manifold, together with

the simulations done with the parameters reported in Table 4. The hyperfine couplings are found to be strong, *i.e.* the signals are centered around $^{N}A/2$ and split over twice the ^{14}N Larmor frequency, with the nuclear quadrupole coupling leading to further broadening of the lines. In Figure 7, only the high-frequency branch is shown. The corresponding ^{14}N nuclear frequencies of the M_S = 1/2 manifold are partially covered by the central Lorentzian hole of the EDNMR spectra as well as contributions of the ^{63,65}Cu hyperfine lines (at observer positions corresponding with g_x and g_y, see exemplary spectrum Figure S15). The assignment of the lines in Figure 7 to ^{14}N could be done based on a number of spectra in which both branches were clearly resolved (see example in Figure S16). The higher *g*-tensor anisotropy detected in the CW X-band EPR spectra is reflected in the broader and asymmetric high-field peak of the W-band ESE detected EPR spectrum of [Cu(**PrHSS**)]$^{2-}$ corresponding with the g_x and g_y parameters (Figure 6b, Table S4).

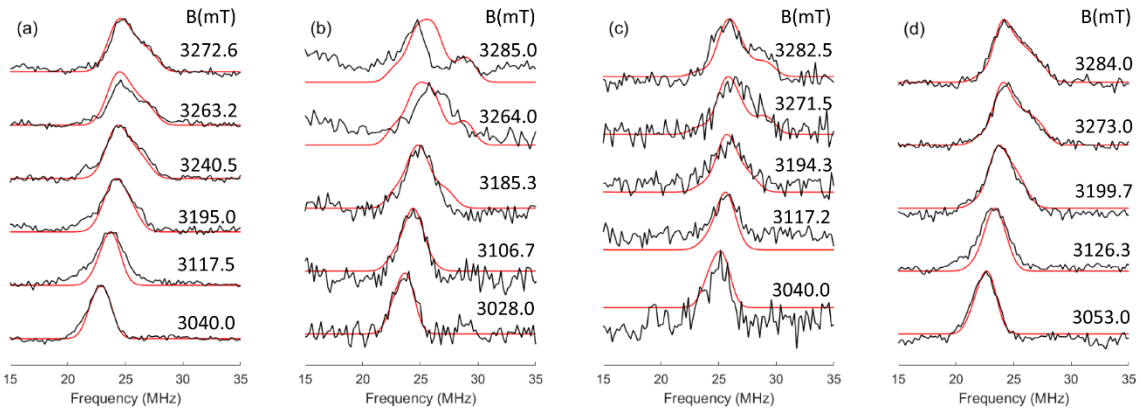

Figure 7. Experimental (black) and simulated (red) W-band ^{14}N EDNMR spectra recorded at 6 K for 80% water/glycerol solutions of the complexes (a) [Cu(**HSS**)]$^{2-}$ (b) [Cu(**PrHSS**)]$^{2-}$ (c) [Cu(**BuHSS**)]$^{2-}$ and (d) [Cu(*cis*-**CyHSS**)]$^{2-}$ recorded at different magnetic-field settings. Only the features of the high-frequency branch of the ^{14}N nuclear transitions (M_S=-1/2 manifold) are shown. A detailed explanation is given in the main text. The simulations are done using the values reported in Table 4.

Table 4. Nitrogen hyperfine and quadrupole values (in MHz) used in the simulation of the W-band EDNMR shown in Figure 7.

Complex	^{14}N	A_x	A_y	A_z	Q_x	Q_y	Q_z	$^{N}A_0 = \frac{\sum_{i=1}^{3} A_i}{3}$
[Cu(**HSS**)]$^{2-}$	N1[a)]	32.0	30.0	25.5	-1.20	0.73	0.47	29.2
	N2[b)]	31.0	26.0	25.5	-1.20	0.73	0.47	27.5
[Cu(**PrHSS**)]$^{2-}$	N1[c)]	36.0	27.0	28.0	-1.0	0.60	0.40	30.3
	N2[d)]	36.0	26.5	28.0	-1.0	0.60	0.40	30.2
[Cu(**BuHSS**)]$^{2-}$	N1[a)]	35.0	32.0	31.0	-1.20	0.73	0.47	32.7
	N2[b)]	32.0	28.0	31.0	-1.20	0.73	0.47	30.3
[Cu(*cis*-**CyHSS**)]$^{2-}$	N1[a)]	32.0	30.0	25.5	-1.20	0.73	0.47	29.2
	N2[b)]	31.0	26.0	25.5	-1.20	0.73	0.47	27.5

Euler angles for both A and Q are: a) α=45°±10°, β,γ = 0°±10°, b) α=-45°±10°, β,γ = 0°±10°; c) α=50°±15°, β,γ = 0°±15°, d) α=-50°±15°, β,γ = 50°±15°. The experimental error was ± 1 MHz for A_x, ±1.5 MHz for A_y, ±1 MHz for A_z and ± 0.3 MHz for **Q**.

From Table 4, a clear difference is observed between the hyperfine values of [Cu(**HSS**)]$^{2-}$ and [Cu(*cis*-**HSS**)]$^{2-}$, on the one hand, and [Cu(**PrHSS**)]$^{2-}$ and [Cu(**BuHSS**)]$^{2-}$ on the other hand. Moreover, the spin density on the nitrogen nuclei is also increased in the latter case, as follows from the increase in the ^{14}N isotropic hyperfine contribution ($^{N}A_0$). Smaller spin density on the nitrogen nuclei results from a smaller overlap between the N orbitals and the $d_{x^2-y^2}$ orbital of copper, pointing to a less planar (CuONNO) segment. The difference observed here between

the two sets of copper complexes suggests a higher tension induced by the bridging fragment in the (6,5) membered chelates versus the (6,6) and (6,7) membered chelates. The overall ^{14}N spin density for the studied complexes (and hence the ^{14}N hyperfine values) is only 65-80% of the earlier reported spin density on the imine nitrogens in related Cu(II) salen complexes [15] This can be related to the difference between the imine and amine nitrogens (difference between the sp^2 and sp^3 hybridization of the copper-ligating nitrogen) and, to a lesser extent, to the higher planarity in the salen case. This is substantiated by the observation that the ^{14}N spin density of the here-studied Cu(II) salan complexes is also 60-70% of the one reported for copper complexes of phenolic oximes, of which some have slight tetrahedral distortion.[46] [47] Similarly the ^{14}N isotropic hyperfine values of the pyrrole nitrogens in planar copper porphyrins and copper phthalocyanines are significantly larger than those of the Cu(II) salan complexes in this study.[48]

These values are however close to those obtained for amino nitrogen (-NH_2) couplings of copper(II) – dipeptides determined by EDNMR ($^{N}A_0$ = 32.0 – 32.3 MHz). [49] Furthermore, while the hyperfine values of the imine nitrogens in Cu(II) salen complexes are indistinguishable,[15] the values of the two ligating amine nitrogens in the Cu(II) salan complexes are slightly different (Table 4), indicating small local out-of-plane distortions.

The complex formation processes were examined at different pH's in frozen solution in case of **HSS**, **PrHSS** and **BuHSS** (Figures S17-S19). Around pH ~ 4 only $[Cu(aqua)]^{2+}$ complex was found both for **HSS** and **PrHSS** ligands. The protonated $[Cu(LH)]^{-}$ complex could be detected for **HSS** in addition to the $[Cu(aqua)]^{2+}$ complex at pH = 4.50. At pH = 11.0 the same signal was measured as at pH = 7.0, thus the formation of mixed hydroxido complex was detected neither under the conditions of EPR spectroscopy nor during the pH-potentiometric titrations. For Cu(II)/**PrHSS**, the spectrum measured at pH = 5.39 can be fitted well with consideration of two components in the simulation. These components are the $[Cu(\mathbf{PrHSS})]^{2-}$ complex and

presumably an unidentified copper(II) complex possessing a broad singlet spectrum. This is usually due to the line broadening effect of close copper centres originating from dimer complexes or precipitations. At pH = 7.0 the signal can be fitted with one component ([Cu(**PrHSS**)]$^{2-}$) and the same spectrum is preserved at pH = 11.46. In case of **BuHSS** the same [Cu(**BuHSS**)]$^{2-}$ spectra were recorded for all the three investigated pH's (7.0, 8.02 and 11.52).

Synthesis of Cu(II)-sulfosalan complexes in solid form and their catalytic application in the Henry reaction. The copper(II) complexes of sulfonated salan ligands were obtained in a straightforward method by heating equimolar amounts of $Cu(OAc)_2$ and the appropriate ligand (L) in basic aqueous solution. Depending on the ligand, the pH was adjusted to 7.0 – 8.5 at which – according to the equilibrium measurements – all the Cu(II) ions were found in form of $[Cu(L)]^{2-}$. Precipitation with cold ethanol and subsequent washings furnished the solid products as bluish-green or blue solids in 59-82% yields. HR ESI mass spectra were in excellent agreement with the calculated masses of the respective ions. In the FTIR spectra, all complexes exhibited the characteristic strong absorptions of the $-SO_3^-$ group around 1030 and 1180 cm^{-1}, while the absorptions in the 1155 ± 15 cm^{-1} range can be likely assigned to the Ar–O vibrations. UV-vis and EPR spectral features are discussed in the previous sections of this manuscript.

Several attempts were made to obtain single crystals suitable for X-ray diffraction measurements, however, these were mostly unsuccessful. The notable exception was [Cu(**PrHSS**)]$^{2-}$, single crystals which were obtained from a KOH solution as K_2[Cu(**PrHSS**)]×3H_2O. Details on this structure are reported in the Supporting Information.

Catalysis of the Henry reaction by copper(II)-sulfosalan complexes in aqueous media. The reaction of nitroalkanes with aldehydes or ketones is a synthetically useful reaction resulting in β-nitro alcohols which can yield important compounds upon further transformations (e.g. nitroalkenes by dehydration or β-amino alcohols via reduction). [16, 17, 18,50, 51]The reaction is catalyzed by various bases, however, transition metal catalysts are used increasingly, especially

for enantioselective synthesis of β-nitro alcohols. Copper complexes were found to be effective catalysts in this reaction.[19] [52] [53] [20] [54]The Henry reaction of benzaldehyde with nitromethane (Scheme 2) is often studied to establish the basic catalytic properties of new types of catalysts.[55,56,57]

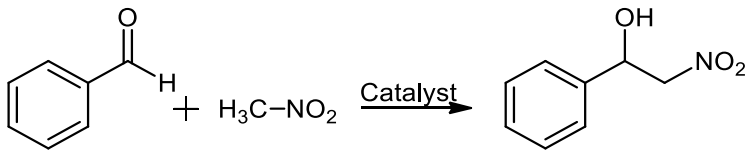

Scheme 2. Henry reaction of benzaldehyde and nitromethane.

We have established, that in aqueous solution, the various Cu(II)-sulfosalan complexes efficiently catalyzed the reaction of benzaldehyde and nitromethane under mild conditions and in air. According to the ^{1}H NMR spectra of the reaction mixtures, the reactions yielded the corresponding nitroaldol product exclusively, and only unreacted starting compounds could be observed in addition (Figure S26). The originally blue solutions of the Cu(II)-sulfosalans gradually turned to yellow and later orange or light brown. However, the reaction mixtures regained their blue colour upon standing (in air). No changes in the conversions were observed when the reactions were run in an argon atmosphere. The conversions were not affected by addition of trimethylamine, either, showing that it did not act as a base catalyst or a ligand for Cu(II). Table 5 shows the yield of the reaction with the various catalysts as a function of time (see also Figure S27).

Table 5. Yield of the nitroaldol product in Henry reaction of benzaldehyde with nitromethane with various catalysts as a function of time. [a]

Catalyst	*Reaction time (h)*			
	4	12	19	36
	Yield (%)			
No Cu(II)	8	10	15	15
$Cu(OAc)_2$	9	15	19	36
Na_2[Cu(**HSS**)] (**1**)	9	16	21	31
Na_2[Cu(**PrHSS**)] (**2**)	14	25	26	43
Na_2[Cu(**BuHSS**)] (**3**)	19	20	34	46
Na_2[Cu(**dPhHSS**)] (**6**)	23	26	36	50

[a] *Conditions*: 0.5 mmol benzaldehyde, 2.5 mmol nitromethane, 5 mol% Cu(II) catalyst, 2 mL water, 75 °C

There was a slow reaction in the absence of a Cu(II) catalyst, too, and $Cu(OAc)_2$ itself also showed appreciable catalytic activity. While the activity of Na_2[Cu(**HSS**)] (**1**) was equal to or only slightly higher than that of $Cu(OAc)_2$, the Na_2[Cu(**PrHSS**)] (**2**), Na_2[Cu(**BuHSS**)] (**3**), and Na_2[Cu(**dPhHSS**)] (**6**) catalysts showed significantly higher activity. The best result, 50 % yield corresponding to TON = 10 (TON = turnover number = (mol reacted benzaldehyde)(mol catalyst)$^{-1}$) was obtained with Na_2[Cu(**dPhHSS**)] (**6**) in 36 h at 75 °C. This catalytic activity is close to that (TON = 14) determined in the same reaction under identical conditions for Cu(II)-tris(pyrazolylmethane) sulfonate complexes, [57] but lags behind the activity (up to TON 67.3 in 48 h) of the copper(II) catalysts bearing a sulfonated Schiff base ligand 2-(2-pyridylmethyleneamino)benzenesulfonate.[55] Aqueous solutions of the isolated Cu(II)-sulfosalan complexes used here for catalytic studies, have a pH around 8. According to the pH-potentiometric investigations, above pH 8, all copper is in form of $[Cu(L)]^{2-}$ with each studied sulfosalan ligand. Consequently, we attribute the catalytic activities determined in the above reactions exclusively to $[Cu(L)]^{2-}$ complexes with no contribution from other possible forms of Cu(II) which – in principle – could be obtained by dissociation of L. The effect of the pH on the catalytic activity was studied in the reaction between benzaldehyde and nitromethane with Na_2[Cu(**dPhHSS**)] as the catalyst. The results are shown in Figure 8, which also displays the

species distribution in the Cu(II)/**dPhHSS** system as a function of pH. As can be seen, by increasing the mole fraction of [Cu(**dPhHSS**)]$^{2-}$ (e.g. increasing the pH), the yield of the nitroaldol product increases parallel and levels off at pH = 6 when all Cu(II) ions are already bounded to the **dPhHSS**. On the basis of this result, it may be concluded that under neutral or basic conditions all catalysis can be attributed to [Cu(**dPhHSS**)]$^{2-}$.

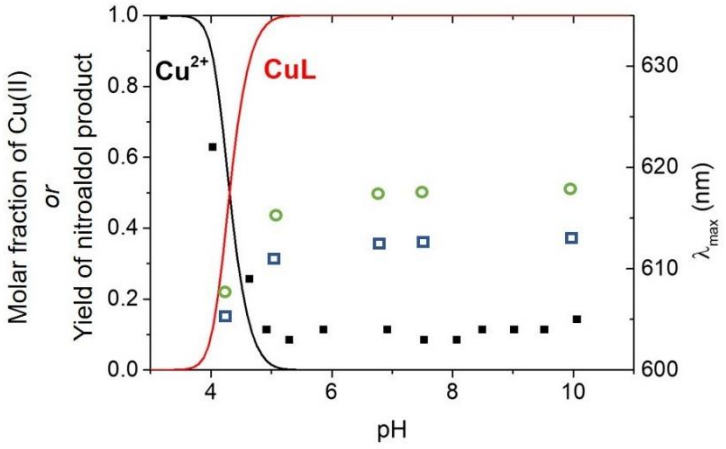

Figure 8. Distribution of the complexes formed in the Cu(II)/**dPhHSS** 1/1 systems and the λ_{max} values at the *d-d* band (■) obtained by UV-vis spectroscopy as a function of pH (c_L = 2 mM, T = 298 K). The open symbols (□ and ○) represent the yield of the nitroaldol product in the Henry reaction of benzaldehyde and nitromethane after 19 h and 36 h, respectively. Yields are expressed as mole fractions of the initial benzaldehyde amount (conditions of the catalytic reaction: 0.5 mmol benzaldehyde, 2.5 mmol nitromethane, 0.025 mmol Na_2[Cu(**dPhHSS**)], 2 mL water, 75 °C).

The Na_2[Cu(**PrHSS**)] (**2**) complex was also applied as catalyst for the Henry reaction of nitromethane with other aldehydes, too (Table 6). While the 4-bromo-, 4-fluoro-, and 2-ethoxy substituents changed the reactivity of the respective benzaldehyde only slightly, the conversion of *m*-tolualdehyde was only one fifth of that of the parent benzaldehyde.

Table 6. Henry reaction of nitromethane with various benzaldehydes catalyzed by Na_2[Cu(**PrHSS**)] (**2**) in aqueous media. a

Aldehyde	Yield (%)
Benzaldehyde	26
4-Bromobenzaldehyde	29
4-Fluorobenzaldehyde	18
2-Ethoxybenzaldehyde	21
3-Methylbenzaldehyde	5

[a] *Conditions*: 0.5 mmol benzaldehyde, 2.5 mmol nitromethane, 5 mol% catalyst, 2 mL water, 75 °C, 19 h.

The size of the nitroalkane chain also affected the yield. In the reaction of nitropropane and benzaldehyde, with the use of 5 mol% of Na_2[Cu(**PrHSS**)] catalyst at 75°C in 19 hours reaction time, only 20% nitroaldol yield (*anti*:*syn* molar ratio 44:56) was obtained instead of 26 % with nitromethane.

Henry reactions between benzaldehyde and nitromethane were also performed with *in situ* prepared Cu(II)-sulfosalan catalysts. For this purpose, equimolar amounts of Cu(II)-acetate and the appropriate sulfosalan ligand were heated in water for 2 h and aliquots of the resulting blue solutions were used for catalysis. Comparison of the benzaldehyde conversions obtained with the *in situ* prepared or the isolated complexes showed similar catalytic activities in the two cases (e.g. for Na_2[Cu(**PrHSS**)] in 19 h: 26 % - isolated catalyst; 20 % - *in situ* prepared catalyst).

In liquid biphasic catalytic systems, the addition of water-miscible organic co-solvents to the aqueous phase may be necessary to facilitate mass transport between the organic phase of a water-insoluble organic substrate and the catalyst-containing aqueous phase. With the use of water/methanol 1/1 (v/v) mixtures as solvent, we observed no effect on the conversion of benzaldehyde-nitromethane nitroaldol reaction with Na_2[Cu(**HSS**)] (**1**) and Na_2[Cu(**PrHSS**)] (**2**) catalysts, however, in the case of Na_2[Cu(**BuHSS**)] (**3**) and Na_2[Cu(**dPhHSS**)] (**6**) the conversions fell significantly (33 to 27 %, and 36 to 25 %, respectively) (Figure S28). In a

related study using Cu(II)-complexes of a sulfonated Schiff base ligand as catalysts, it was also found, that Henry reactions proceeded faster in water than in methanol.[55] Since the general mechanism of the Henry reaction includes deprotonation/protonation steps,[18] and it is assisted by strong hydrogen bonding in aqueous solutions, [20] the beneficial effect of water on the reaction rate can be rationalized by the high polarity, high proton solvation power of water, and propensity for hydrogen bond formation.

CONCLUSIONS

In summary, solution equilibria, spectroscopic and catalytic features of copper(II) sulfosalan complexes were studied with the use of pH-potentiometry and several spectroscopic methods. All the investigated ligands form mononuclear complexes with copper(II) and the metal ion is accommodated by the (O^-,N,N,O^-) donor set. This coordination mode is dominant in the entire pH-range and hinders the formation of mixed hydroxido species. The investigated ligands exhibit a trend of copper(II) ion affinity which is as follows: *trans*-**CyHSS** > *cis*-**CyHSS** > **HSS** > **dPhHSS** > **PrHSS** > **BuHSS**.

The copper(II) complexes possess square-planar coordination environment, however, higher rhombicity was detected for **PrHSS** than for the other species. On the basis of g_z and λ_{max} values of the complexes, a decreasing of the ligand field was observed in the order: **dPhHSS** > *cis*-**CyHSS** > **BuHSS** ~ **HSS** > **PrHSS**. The *trans*-**CyHSS** gave an outlier value and exhibits the highest ligand field.

The Cu(II)-sulfosalan complexes were found catalytically active in the Henry (nitroaldol) reaction between benzaldehyde and nitromethane. Water-solubility of the Cu(II)-complex catalysts allowed using water as the only solvent in the reaction, in accord with the pursuit of reducing organic solvents' use in chemical procedures.

Finally, our results unambiguously show that multidisciplinary approach is necessary to design new homogeneous catalysts. The combination of solution equilibrium and sensitive

spectroscopic techniques such as EPR provides deeper insight into the thermodynamic and electronic features of copper(II) complexes which can influence the activity of putative catalysts. In our case, the high thermodynamic stability and symmetric square-planar geometry are not favorable to catalyze effectively the nitroaldol reaction between aldehydes and nitromethane, however, moderate stability, rhombic coordination geometry and higher spin density on the N nucleus may contribute to increase their efficiency. The Henry reaction includes the simultaneous binding of the electrophile and nucleophile to the metal center. For the most reactive transition state, the nucleophile should be placed perpendicular to the ligand plane (axial positions) while the electrophile should occupy in one of the more Lewis acidic equatorial sites. [58] For the sulfosalan complexes, the donor groups are located in the equatorial positions, therefore those copper(II) complexes which exhibit higher rhombicity and small local out-of-plane distortions (e.g. copper(II) complexes **PrHSS** or **BuHSS**) may provide better environment to accommodate the reactants.

ASSOCIATED CONTENT

Supporting Information

The Supporting Information is available free of charge at…..

Synthesis and isolation of the Cu(II)-sulfosalan complexes, scheme of the deprotonation microprocesses, distribution curves, MS spectra and measured and calculated m/z values, table of absorption maxima and molar absorption coefficient of the copper(II) complexes, experimental and calculated CW-EPR spectra and their simulated parameters, W-ban ESE detected EPR spectra, W-band EDNMR spectra, frozen solution X-ban CW-EPR spectra, ORTEP diagram, crystal data, yields of nitroaldol production.

Author Information

Corresponding Authors

Nóra V. May – Research Centre for Natural Sciences, Budapest, Hungary; E-mail: may.nora@ttk.mta.hu

Ferenc Joó – Department of Physical Chemistry, MTA-DE Redox and Homogeneous Reaction Mechanisms Research Group, University of Debrecen, Debrecen, Hungary; E-mail: joo.ferenc@science.unideb.hu

Norbert Lihi – Department of Inorganic and Analytical Chemistry, MTA-DE Redox and Homogeneous Reaction Mechanisms Research Group, University of Debrecen, Debrecen, Hungary; E-mail: lihi.norbert@science.unideb.hu

Authors

Szilvia Bunda – Department of Physical Chemistry, Doctoral School of Chemistry, University of Debrecen, Debrecen, Hungary

Dóra Bonczidai-Kelemen – Department of Inorganic and Analytical Chemistry, Doctoral School of Chemistry, University of Debrecen, Debrecen, Hungary

Antal Udvardy – Department of Physical Chemistry, University of Debrecen, Debrecen, Hungary

H. Y. Vincent Ching – Department of Chemistry, University of Antwerp, Antwerpen, Belgium

Kevin Nys – Department of Chemistry, University of Antwerp, Antwerpen, Belgium

Mohammad Samanipour – Department of Chemistry, University of Antwerp, Antwerpen, Belgium

Sabine Van Doorslaer – Department of Chemistry, University of Antwerp, Antwerpen, Belgium

Author Contributions

The manuscript was written through contributions of all authors. All authors have given approval to the final version of the manuscript.

Notes

The authors declare no competing financial interest and there are no conflicts to declare.

ACKNOWLEDGEMENTS

This research was funded by the EU and co-financed by the European Regional Development Fund (under the projects GINOP-2.3.2-15-2016-00008 and GINOP-2.3.3-15-2016-00004), and the Thematic Excellence Programme (TKP2020-NKA-04) of the Ministry for Innovation and Technology in Hungary. The financial support of the Ministry for Innovation and Technology from the source of the National Research, Development and Innovation Found (FK-128333, K-124544 and PD-128326) is gratefully acknowledged. N. L. is indebted to the New National Excellence Program of the Ministry for Innovation and Technology from the source of the National Research, Development and Innovation Found (ÚNKP-20-4-II).

S.V.D. and N.V.M is grateful for the fund of FWO-MTA mobility grant (contract No. PROJEKT17-16).

This work is prepared with the professional support of the Doctoral Student Scholarship Program of the Co-operative Doctoral Program of the Ministry of Innovation and Technology financed from the National Research, Development and Innovation Office.

REFERENCES

1. Gupta, K. C.; Sutar, A. K. Catalytic activities of Schiff base transition metal complexes. *Coordination Chemistry Reviews* **2008,** 252 (12), 1420-1450.
2. Correia, I.; Pessoa, J. C.; Duarte, M. T.; da Piedade, M. F. M.; Jackush, T.; Kiss, T.; Castro, M. M. C. A.; Geraldes, C. F. G. C.; Avecilla, F. Vanadium(IV and V) Complexes of Schiff Bases and Reduced Schiff Bases Derived from the Reaction of Aromatic o-Hydroxyaldehydes and Diamines: Synthesis, Characterisation and Solution Studies. *European Journal of Inorganic Chemistry* **2005,** 2005 (4), 732-744.
3. Shahnaz, N.; Puzari, A.; Paul, B.; Das, P. Activation of aryl chlorides in water for Suzuki coupling with a hydrophilic salen-Pd(II) catalyst. *Catalysis Communications* **2016,** 86, 55-58.
4. Sippola, V. O.; Krause, A. O. I. Oxidation activity and stability of homogeneous cobalt-sulphosalen catalyst: Studies with a phenolic and a non-phenolic lignin model compound in aqueous alkaline medium. *Journal of Molecular Catalysis A: Chemical* **2003,** 194 (1), 89-97.

5. Talsi, E. P.; Bryliakov, K. P. Ti-Salan catalyzed asymmetric sulfoxidation of pyridylmethylthiobenzimidazoles to optically pure proton pump inhibitors. *Catalysis Today* **2017,** 279, 84-89.
6. Wang, X.; Wu, G.; Wang, F.; Ding, K.; Zhang, F.; Liu, X.; Xue, Y. Base-free selective oxidation of glycerol with 3% H2O2 catalyzed by sulphonato-salen-chromium(III) intercalated LDH. *Catalysis Communications* **2012,** 28, 73-76.
7. Whiteoak, C. J.; Torres Martin de Rosales, R.; White, A. J. P.; Britovsek, G. J. P. Iron(II) Complexes with Tetradentate Bis(aminophenolate) Ligands: Synthesis and Characterization, Solution Behavior, and Reactivity with O2. *Inorganic Chemistry* **2010,** 49 (23), 11106-11117.
8. Pessoa, J. C.; Correia, I. Salan vs. salen metal complexes in catalysis and medicinal applications: Virtues and pitfalls. *Coordination Chemistry Reviews* **2019,** 388, 227-247.
9. Lihi, N.; Bunda, S.; Udvardy, A.; Joó, F. Coordination chemistry and catalytic applications of Pd(II)–, and Ni(II)–sulfosalan complexes in aqueous media. *Journal of Inorganic Biochemistry* **2020,** 203, 110945.
10. Bunda, S.; Voronova, K.; Kathó, Á.; Udvardy, A.; Joó, F. Palladium (II)–Salan Complexes as Catalysts for Suzuki–Miyaura C–C Cross-Coupling in Water and Air. Effect of the Various Bridging Units within the Diamine Moieties on the Catalytic Performance. *Molecules* **2020**, 3993.
11. Adão, P.; Barroso, S.; Avecilla, F.; Oliveira, M. C.; Pessoa, J. C. CuII–salan compounds: Synthesis, characterization and evaluation of their potential as oxidation catalysts. *Journal of Organometallic Chemistry* **2014,** 760, 212-223.
12. Bunda, S.; Udvardy, A.; Voronova, K.; Joó, F. Organic Solvent-Free, Pd(II)-Salan Complex-Catalyzed Synthesis of Biaryls via Suzuki–Miyaura Cross-Coupling in Water and Air. *The Journal of Organic Chemistry* **2018,** 83 (24), 15486-15492.
13. Voronova, K.; Purgel, M.; Udvardy, A.; Bényei, A. C.; Kathó, Á.; Joó, F. Hydrogenation and Redox Isomerization of Allylic Alcohols Catalyzed by a New Water-Soluble Pd–tetrahydrosalen Complex. *Organometallics* **2013,** 32 (15), 4391-4401.
14. Voronova, K.; Homolya, L.; Udvardy, A.; Bényei, A. C.; Joó, F. Pd–Tetrahydrosalan-Type Complexes as Catalysts for Sonogashira Couplings in Water: Efficient Greening of the Procedure. *ChemSusChem* **2014,** 7 (8), 2230-2239.
15. Murphy, D. M.; Caretti, I.; Carter, E.; Fallis, I. A.; Göbel, M. C.; Landon, J.; Doorslaer, S. V.; Willock, D. J. Visualizing Diastereomeric Interactions of Chiral Amine–Chiral Copper Salen Adducts by EPR Spectroscopy and DFT. *Inorganic Chemistry* **2011,** 50 (15), 6944-6955.
16. Ballini, R.; Bosica, G. Nitroaldol Reaction in Aqueous Media: An Important Improvement of the Henry Reaction. *The Journal of Organic Chemistry* **1997,** 62 (2), 425-427.
17. Luzzio, F. A. The Henry reaction: recent examples. *Tetrahedron* **2001,** 57 (6), 915-945.
18. Kürti, L.; Czakó, B. *Strategic Applications of Named Reactions in Organic Synthesis*. Academic Press: Cambridge, UK, 2005; p 864.
19. Chougnet, A.; Woggon, W.-D. In *Organic Syntheses*; pp 52-61.
20. Jammi, S.; Ali, M. A.; Sakthivel, S.; Rout, L.; Punniyamurthy, T. Synthesis, Structure, and Application of Self-Assembled Copper(II) Aqua Complex by H-Bonding for Acceleration of the Nitroaldol Reaction on Water. *Chemistry – An Asian Journal* **2009,** 4 (2), 314-320.
21. Gran, G. Determination of the equivalence point in potentiometric titrations. Part II. *Analyst* **1952,** 77 (920), 661-671.
22. Irving, H. M.; Miles, M. G.; Pettit, L. D. A study of some problems in determining the stoicheiometric proton dissociation constants of complexes by potentiometric titrations using a glass electrode. *Analytica Chimica Acta* **1967,** 38, 475-488.
23. Gans, P.; Sabatini, A.; Vacca, A. SUPERQUAD: an improved general program for computation of formation constants from potentiometric data. *Journal of the Chemical Society, Dalton Transactions* **1985,** (6), 1195-1200.

24. Zékány, L.; Nagypál, I. *Computational Methods for the Determination of Formation Constants*. Plenum Press: New York, NY, USA, 1985.
25. *Hydra/Medusa Chemical Equlilibrium Database and Plotting Software, K. R. I. o. T., 2004 http://www.kemi.kth.se/medusa/ freely downloadable software at. I. Puigdomenech.*
26. Rockenbauer, A.; Korecz, L. Automatic computer simulations of ESR spectra. *Applied Magnetic Resonance* **1996,** 10 (1), 29-43.
27. Schosseler, P.; Wacker, T.; Schweiger, A. Pulsed ELDOR detected NMR. *Chemical Physics Letters* **1994,** 224 (3), 319-324.
28. Cox, N.; Nalepa, A.; Lubitz, W.; Savitsky, A. ELDOR-detected NMR: A general and robust method for electron-nuclear hyperfine spectroscopy? *Journal of Magnetic Resonance* **2017,** 280, 63-78.
29. Stoll, S.; Schweiger, A. EasySpin, a comprehensive software package for spectral simulation and analysis in EPR. *Journal of Magnetic Resonance* **2006,** 178 (1), 42-55.
30. Sheldrick, G. SHELXT - Integrated space-group and crystal-structure determination. *Acta Crystallographica Section A* **2015,** 71 (1), 3-8.
31. Sheldrick, G. Crystal structure refinement with SHELXL. *Acta Crystallographica Section C* **2015,** 71 (1), 3-8.
32. Dolomanov, O. V.; Bourhis, L. J.; Gildea, R. J.; Howard, J. A. K.; Puschmann, H. OLEX2: a complete structure solution, refinement and analysis program. *Journal of Applied Crystallography* **2009,** 42 (2), 339-341.
33. Spek, A. checkCIF validation ALERTS: what they mean and how to respond. *Acta Crystallographica Section E* **2020,** 76 (1), 1-11.
34. Macrae, C. F.; Bruno, I. J.; Chisholm, J. A.; Edgington, P. R.; McCabe, P.; Pidcock, E.; Rodriguez-Monge, L.; Taylor, R.; van de Streek, J.; Wood, P. A. Mercury CSD 2.0 - new features for the visualization and investigation of crystal structures. *Journal of Applied Crystallography* **2008,** 41 (2), 466-470.
35. Noël, S.; Perez, F.; Pedersen, J. T.; Alies, B.; Ladeira, S.; Sayen, S.; Guillon, E.; Gras, E.; Hureau, C. A new water-soluble Cu(II) chelator that retrieves Cu from Cu(amyloid-β) species, stops associated ROS production and prevents Cu(II)-induced Aβ aggregation. *Journal of Inorganic Biochemistry* **2012,** 117, 322-325.
36. Lavanant, H.; Virelizier, H.; Hoppilliard, Y. Reduction of copper(ii) complexes by electron capture in an electrospray ionization source. *Journal of the American Society for Mass Spectrometry* **1998,** 9 (11), 1217-1221.
37. Gažo, J.; Bersuker, I. B.; Garaj, J.; Kabešová, M.; Kohout, J.; Langfelderová, H.; Melník, M.; Serator, M.; Valach, F. Plasticity of the coordination sphere of copper(II) complexes, its manifestation and causes. *Coordination Chemistry Reviews* **1976,** 19 (3), 253-297.
38. Sciortino, G.; Maréchal, J.-D.; Fábián, I.; Lihi, N.; Garribba, E. Quantitative prediction of electronic absorption spectra of copper(II)–bioligand systems: Validation and applications. *Journal of Inorganic Biochemistry* **2020,** 204, 110953.
39. Pratt, R. C.; Lyons, C. T.; Wasinger, E. C.; Stack, T. D. P. Electrochemical and Spectroscopic Effects of Mixed Substituents in Bis(phenolate)–Copper(II) Galactose Oxidase Model Complexes. *Journal of the American Chemical Society* **2012,** 134 (17), 7367-7377.
40. Lever, A. B. P. *Inorganic electronic spectroscopy*. Elsevier: London, 1984; Vol. 33.
41. Klement, R.; Stock, F.; Elias, H.; Paulus, H.; Pelikán, P.; Valko, M.; Mazúr, M. Copper(II) complexes with derivatives of salen and tetrahydrosalen: a spectroscopic, electrochemical and structural study. *Polyhedron* **1999,** 18 (27), 3617-3628.
42. Roy, S.; Banerjee, A.; Lima, S.; Horn Jr, A.; Sampaio, R. M. S. N.; Ribeiro, N.; Correia, I.; Avecilla, F.; Carvalho, M. F. N. N.; Kuznetsov, M. L.; Pessoa, J. C.; Kaminsky, W.; Dinda,

R. Unusual chemistry of Cu(ii) salan complexes: synthesis, characterization and superoxide dismutase activity. *New Journal of Chemistry* **2020,** 44 (27), 11457-11470.
43. Gama, S.; Mendes, F.; Marques, F.; Santos, I. C.; Carvalho, M. F.; Correia, I.; Pessoa, J. C.; Santos, I.; Paulo, A. Copper(II) complexes with tridentate pyrazole-based ligands: synthesis, characterization, DNA cleavage activity and cytotoxicity. *Journal of Inorganic Biochemistry* **2011,** 105 (5), 637-644.
44. Peisach, J.; Blumberg, W. E. Structural implications derived from the analysis of electron paramagnetic resonance spectra of natural and artificial copper proteins. *Archives of Biochemistry and Biophysics* **1974,** 165 (2), 691-708.
45. Sakaguchi, U.; Addison, A. W. Spectroscopic and redox studies of some copper(II) complexes with biomimetic donor atoms: implications for protein copper centres. *Journal of the Chemical Society, Dalton Transactions* **1979,** (4), 600-608.
46. Healy, M. R.; Carter, E.; Fallis, I. A.; Forgan, R. S.; Gordon, R. J.; Kamenetzky, E.; Love, J. B.; Morrison, C. A.; Murphy, D. M.; Tasker, P. A. EPR/ENDOR and Computational Study of Outer Sphere Interactions in Copper Complexes of Phenolic Oximes. *Inorganic Chemistry* **2015,** 54 (17), 8465-8473.
47. Moons, H.; Łapok, Ł.; Loas, A.; Van Doorslaer, S.; Gorun, S. M. Synthesis, X-ray Structure, Magnetic Resonance, and DFT Analysis of a Soluble Copper(II) Phthalocyanine Lacking C−H Bonds. *Inorganic Chemistry* **2010,** 49 (19), 8779-8789.
48. Greiner, S. P.; Rowlands, D. L.; Kreilick, R. W. EPR and ENDOR study of selected porphyrin- and phthalocyanine-copper complexes. *The Journal of Physical Chemistry* **1992,** 96 (23), 9132-9139.
49. Nagy, N. V.; Doorslaer, S. V.; Szabó-Plánka, T.; Rompaey, S. V.; Hamza, A.; Fülöp, F.; Tóth, G. K.; Rockenbauer, A. Copper(II)-Binding Ability of Stereoisomeric cis- and trans-2-Aminocyclohexanecarboxylic Acid–l-Phenylalanine Dipeptides. A Combined CW/Pulsed EPR and DFT Study. *Inorganic Chemistry* **2012,** 51 (3), 1386-1399.
50. Phiasivongsa, P.; Samoshin, V. V.; Gross, P. H. Henry condensations with 4,6-O-benzylidenylated and non-protected d-glucose and l-fucose via DBU-catalysis. *Tetrahedron Letters* **2003,** 44 (29), 5495-5498.
51. Jenner, G. Effect of high pressure on Michael and Henry reactions between ketones and nitroalkanes. *New Journal of Chemistry* **1999,** 23 (5), 525-529.
52. Jammi, S.; Punniyamurthy, T. Synthesis, Structure and Catalysis of Tetranuclear Copper(II) Open Cubane for Henry Reaction on Water. *European Journal of Inorganic Chemistry* **2009,** 2009 (17), 2508-2511.
53. Murugavel, G.; Sadhu, P.; Punniyamurthy, T. Copper(II)-Catalyzed Nitroaldol (Henry) Reactions: Recent Developments. *The Chemical Record* **2016,** 16 (4), 1906-1917.
54. Jammi, S.; Saha, P.; Sanyashi, S.; Sakthivel, S.; Punniyamurthy, T. Chiral binuclear copper(II) catalyzed nitroaldol reaction: scope and mechanism. *Tetrahedron* **2008,** 64 (51), 11724-11731.
55. Hazra, S.; Karmakar, A.; Guedes da Silva, M. d. F. C.; Dlháň, L. u.; Boča, R.; Pombeiro, A. J. L. Sulfonated Schiff base dinuclear and polymeric copper(ii) complexes: crystal structures, magnetic properties and catalytic application in Henry reaction. *New Journal of Chemistry* **2015,** 39 (5), 3424-3434.
56. Mahmoud, A. G.; Guedes da Silva, M. F. C.; Śliwa, E. I.; Smoleński, P.; Kuznetsov, M. L.; Pombeiro, A. J. L. Copper(II) and Sodium(I) Complexes based on 3,7-Diacetyl-1,3,7-triaza-5-phosphabicyclo[3.3.1]nonane-5-oxide: Synthesis, Characterization, and Catalytic Activity. *Chemistry – An Asian Journal* **2018,** 13 (19), 2868-2880.
57. Mahmoud, A. G.; Martins, L. M. D. R. S.; Silva, M. F. C. G. d.; Pombeiro, A. J. L. Hydrosoluble Complexes Bearing Tris(pyrazolyl)methane Sulfonate Ligand: Synthesis, Characterization and Catalytic Activity for Henry Reaction. *Catalysts* **2019,** 9 (7), 611.

58. Evans, D. A.; Seidel, D.; Rueping, M.; Lam, H. W.; Shaw, J.; Downey, C. A new copper acetate-bis(oxazoline)-catalyzed, enantioselective Henry reaction. *Journal of the American Chemical Society* **2003,** 125 42, 12692-3.

For Table of Contents Only

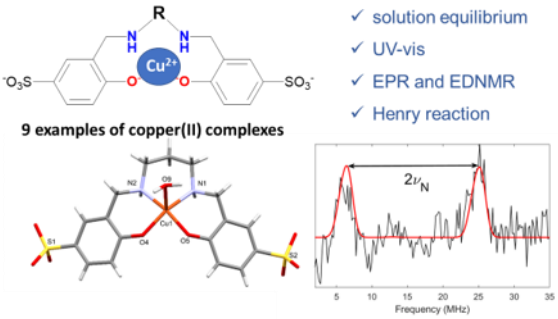

Synopsis

Nine copper(II) complexes were studied using equilibrium and spectroscopic techniques and used as catalyst in the Henry reaction. The results showed that moderate stability, rhombic coordination geometry and higher spin density on the N nucleus contribute to increase the catalytic efficiency of the copper(II) sulfosalan complexes in the Henry reaction.